Hydrazine-Mediated Construction of Nanocrystal Self-Assembly Materials

Ding Zhou, Min Liu, Min Lin, Xinyuan Bu, Xintao Luo, Hao Zhang,* and Bai Yang

State Key Laboratory of Supramolecular Structure and Materials, College of Chemistry, Jilin University, Changchun 130012, PR China

ABSTRACT Self-assembly is the basic feature of supramolecular chemistry, which permits to integrate and enhance the functionalities of nano-objects. However, the conversion of self-assembled structures to practical materials is still laborious. In this work, on the basis of studying one-pot synthesis, spontaneous assembly, and *in situ* polymerization of aqueous semiconductor nanocrystals (NCs), NC self-assembly materials are produced and applied to design high performance white light-emitting diode (WLED). In producing self-assembly materials, the additive hydrazine (N_2H_4) is curial, which acts as the promoter to achieve room-temperature synthesis of aqueous NCs by favoring a reaction-controlled growth, as the polyelectrolyte to weaken inter-NC electrostatic repulsion and therewith facilitate the one-dimensional self-assembly, and in particular as the bifunctional monomers to polymerize with mercapto carboxylic acid-modified NCs *via in situ* amidation reaction. This strategy is versatile for mercapto carboxylic acid-modified aqueous NCs, for example CdS, CdSe, CdTe, $CdSe_xTe_{1-x}$, and $Cd_yHg_{1-y}Te$. Because of the multisite modification with carboxyl, the NCs act as macromonomers, thus producing cross-linked self-assembly materials with excellent thermal, solvent, and photostability. The assembled NCs preserve strong luminescence and avoid unpredictable fluorescent resonance energy transfer, the main problem in design WLED from multiple NC components. These advantages allow the fabrication of NC-based WLED with high color rendering index (86), high luminous efficacy (41 lm/W), and controllable color temperature.

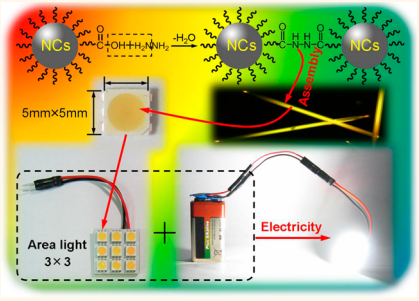

KEYWORDS: quantum dots · self-assembly materials · white light-emitting diode · aqueous synthesis · nanocomposites

Self-assembly architectures composed of inorganic nanocrystals (NCs) have attracted much attention owing to the capability to control NC spatial array and achieve high performance.[1−5] Such self-assembly belongs to supramolecular chemistry that employs various inter-NC weak interactions to construct flexible structures, and thus is expected to promote NC applications in photoelectrics,[6] photovoltaics,[7] catalysis,[8] and bioassay.[9−13] Despite the successes in constructing diversified NC architectures, the weak inter-NC interactions are difficult to maintain structural stability under severe conditions, shedding doubt on conversion of state-of-the-art self-assembly structures to practical materials. The combination of preassembly and *in situ* polymerization of NCs is acceptable to create stable self-assembly architectures and has been demonstrated for reinforcing the assembled NCs at water/oil interfaces to produce stable monolayer.[14] Further methodological expansion and extension will promise the technical applications of NC assemblies in broadening areas.[15]

One promising application of semiconductor NCs is white light-emitting diode (WLED).[16−22] NCs possess broad optical absorption, narrow emission, and good thermal stability.[23−37] In particular, the size-dependent emission and the current success in tailoring NC sizes *via* colloidal chemistry route strongly facilitate the device color control by directly blending the NC components with different emissions.[15,38−47] These make NCs as competitive candidates among various light-emitting materials, for instance organic and polymeric luminescent materials. To date, the performance of NC-based LEDs is limited by the chemical and photostability, concentration quenching, as well as fluorescent resonance energy transfer (FRET) of different NC components.[48] The construction of NC-based WLED highly similar to sunlight is still challenging. Rational self-assembly is capable to arrange NC array and optimize the photoelectric properties, thus high performance WLED is considered to be fabricated using the self-assembly materials of NCs.[49]

Tang and Kotov *et al.* have fabricated the one-dimensional (1D) and 2D self-assembly

* Address correspondence to hao_zhang@jlu.edu.cn.

Received for review July 22, 2014 and accepted October 8, 2014.

Published online October 08, 2014
10.1021/nn5040444

structures from aqueous CdTe NCs by controlling the equilibrium of various inter-NC weak interactions, and proposed the potential application in LEDs.[1,38,49] Eychmüller *et al.* conduct the 1D self-assembly process of CdTe NCs, which further produces a 3D network composed of separated NCs and preseves strong luminescence.[50] However, the conversion of state-of-the-art self-assembled structures to practical materials is still laborious. To produce practical materials, the inter-NC weak attraction should be converted into covalent linkage, so as to maintain structural stability and preserve strong luminescence in device fabrication.[14] The technical difficulty is the *in situ* linkage of the preassembled NCs without altering the emission properties. It requires moderate temperature, proper preassembly and linkage environment, and so forth. The key is to find effective additives, which simultaneously induce NC self-assembly and promote the *in situ* linkage. To design a simple but feasible system, the NC growth kinetics, self-assembly driving forces, as well as polymerization principle must be considered as a whole. We have demonstrated the synthesis of aqueous NCs *via* simple amine-promoted route, for example N_2H_4-participated synthesis of luminescent CdTe NCs at room temperature.[51,52] N_2H_4 is a weak electrolyte, which facilitates the reaction-controlled rapid growth of NCs by creating a favorable electrostatic environment. In addition, the presence of N_2H_4 greatly weakens the inter-NC electrostatic repulsion, and therewith rebuilds the equilibrium of inter-NC interactions.[53] It is expected to direct NC self-assembly following the electrostatic repulsion-conducted process in aqueous media. Furthermore, N_2H_4 possess two amine groups, and can be looked as bifunctional monomers to participate the polymerization with surface-modified NCs under proper conditions. In aqueous NC system, surface modification is not so laborious. Mercapto-compounds are employed as the capping ligands in NC synthesis, directly bestowing NCs with surface carboxyl, hydroxyl, and/or amine.[54] These groups make NCs as macromonomers to participate polymerization.

In the present work, N_2H_4 is employed as the additive to induce the 1D self-assembly of aqueous NCs, and meanwhile as the monomers to polymerize with mercapto carboxylic acid-modified NCs, thus producing NC self-assembly materials with excellent thermal, solvent, and photostability. Because N_2H_4 is also the promoter in NC synthesis, the current method combines the synthesis, preassembly, and *in situ* polymerization of luminescent NCs completely in one pot. Systematic studies confirm that the N_2H_4-mediated preassembly and *in situ* polymerization are extendable to the complexes of mercapto carboxylic acids and Cd^{2+}. This permits to flexibly control the emission color and intensity of NC self-assembly materials by random supplement of NCs with specific concentrations and/or components. Because NCs are already preassembled, concentration quenching and FRET are effectively avoided in further applications. These advantages greatly facilitate the design and fabrication of NC-based LED. A WLED prototype is designed by employing the NC self-assembly materials as color conversion layer. The devices exhibit high color rendering index (CRI, 86), high luminous efficacy (41 lm/W), and controllable color temperature.

RESULTS AND DISCUSSION

In our previous studies about room-temperature one-pot synthesis of semiconductor NCs in aqueous media, N_2H_4 has been proved to promote NC growth.[51] N_2H_4 is a weak electrolyte, which is capable to generate a favorable electrostatic environment and therewith facilitates the reaction-controlled rapid growth of NCs. In addition, inter-NC electrostatic repulsion is the main driving force to maintain the colloidal stability of aqueous NCs. But the large excess N_2H_4 in NC growth solution greatly weakens the inter-NC electrostatic repulsion, thus leading to the poor colloidal stability of the as-synthesized NCs. For example, a spontaneous aggregation and separation of NCs from the growth solution has been observed using 2-mercaptoethylamine (MA) as the capping ligand.[51] Despite the aggregates are redispersible in pure water owing to the noncovalent linkage, this phenomenon inspires us to fabricate stable self-assembly materials by deliberating NC self-assembly driving forces and polymerization principle as a whole. Besides as the promoter in NC growth and the media to induce NC aggregation/assembly, N_2H_4 is further considered to generate *in situ* polymerization of preassembled NCs. In this context, each N_2H_4 possesses two amines that can be looked as bifunctional monomers. Aqueous NCs are looked as macromonomers because of the multisite surface modification with mercapto-compounds. In order to create an amidation reaction with N_2H_4, 3-mercaptopropionic acid (MPA)-modified NCs are employed in the current studies. Following the stepwise polymerization between N_2H_4 and carboxyl-functionalized NCs, cross-linked self-assembly materials are expected to be produced.

CdTe NC Self-Assembly Materials with 1D Orientation. As mentioned in the experimental section, the preparation of NC self-assembly materials involve the storage of NC precursor solution for 48 h and the subsequent N_2H_4-promoted growth for additional 16 h. During the first 48 h, it is the nucleation process of aqueous CdTe NCs, where the amorphous aggregates gradually transform into isolated crystal nucleus (Figure S1, Supporting Information).[55] After the addition of N_2H_4 into crystalline CdTe nucleus, during the rest 16 h, it involves the size increase of NCs and the subsequent formation of self-assembly materials at the bottom of the flask (Figure S2 and S3). Figure 1a indicates the optical photograph of the products, which appear as

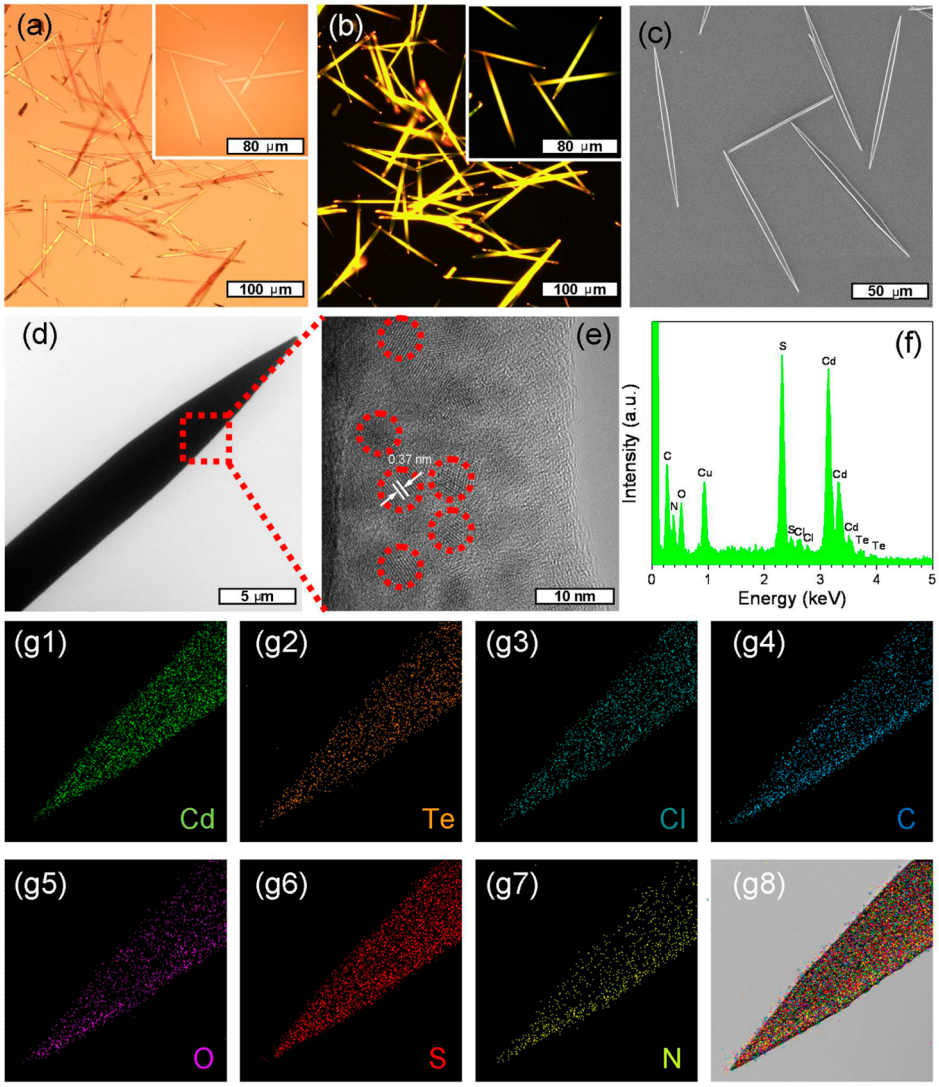

Figure 1. Optical (a), fluorescent (b), SEM (c), TEM (d), and HRTEM (e) images of CdTe NC self-assembly materials. The EDS pattern (f), and mapping images (g1−8) are also shown. Insets: high magnification images.

transparent crystals with 1D orientation. These 1D structures exhibit bright emission under fluorescence microscope (Figure 1b), implying they are composed of luminescent NCs. Scanning electron microscope (SEM) and transmission electron microscopy (TEM) observations reveal that the 1D structures have the average length of 100 μm and width of 5 μm (Figure 1c and d). Energy dispersive spectrum (EDS) and mapping images confirm the existence of Cd and Te elements (Figure 1f, g1 and g2), strongly supporting the component of CdTe NCs. The homogeneous distribution of Cd and Te elements also means that the NCs are well dispersed in the 1D structures rather than form separated phase (Figure 1g1−8). The distance of neighboring NCs is determined according to high-resolution TEM (HRTEM) image (Figure 1e), which is 3.5 nm by measuring 50 neighboring NCs. This further confirms the homogeneous distribution of NCs in the 1D structures. The HRTEM image also indicates that the NCs are well formed single crystals with observed interplanar distance of 0.37 nm, consisting with the (111) crystallographic facet of zinc blende structure of bulk CdTe crystal.[32] However, no characteristic diffraction peaks of CdTe NCs are observed for the X-ray powder diffraction (XRD) pattern (Figure 2a). The situation is much like CdTe-contained $CaCO_3$ crystals, in which the weak diffraction peaks of NCs are completely concealed by those of $CaCO_3$ host (Figure S4). So, the host lattices of 1D structure should not be CdTe. Inductive coupled plasma emission spectrometer (ICP) analysis proves that the content of CdTe NCs is about 20%. In addition, ICP and elemental analysis data indicate that Cd, S, C, and N are the main elements in the 1D structure. This implies that the host of 1D structure is N_2H_4-linked Cd-MPA complexes. This result in return explains why the distance of neighboring NCs is much larger than the length of two MPA. Namely, NCs are not directly linked, but separated by N_2H_4-linked Cd-MPA complexes.

To verify this consideration, N_2H_4 is deliberately added into the mixture of $CdCl_2$ and MPA. After storing

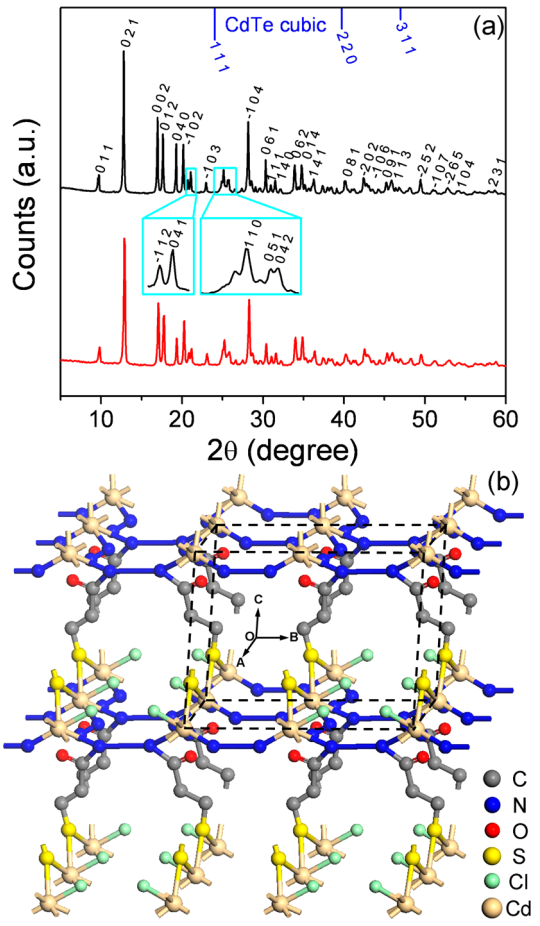

Figure 2. (a) XRD patterns of CdTe-contained (black), and CdTe-free (red) 1D material. (b) The crystalline structure of CdTe-free 1D material. The unit cell is dashed to lead the eye.

the solution at room temperature for 2 h, needlelike products are also observed. The morphology is very similar to the 1D structure composed of CdTe NCs (Figure S5). Importantly, the XRD pattern of CdTe-free 1D structure is the same as that of CdTe-contained samples (Figure 2a). Elemental analysis and ICP data demonstrate that the composition of CdTe-free 1D structure is $CdClSC_3ON_4H_{11}$. PowderX computer program is employed for indexing the XRD patterns and lattice constant calculation.[56] It demonstrates that the 1D structure fits well to a single-phase model corresponding to monoclinic phase, where a = 4.422 Å, b = 18.336 Å, c = 12.749 Å, $\alpha = 90°$, $\beta = 125.5°$, and $\gamma = 90°$ (Figure 2a and Table S1). According to above analysis, one possible crystalline structure is proposed in Figure 2b. This result confirms that the host of 1D structure is cross-linked Cd-MPA complexes. Cd-MPA complexes are converted into rigid network through N_2H_4 linkage, thus forming specific crystal structure. In addition, because CdTe NCs are surface-modified with carboxyl also, the partial replacement of Cd-MPA complexes in the crystals by NCs produces NC-contained 1D structure.

1D-orientated self-assembly of both Cd-mercaptoacetic acid (MAA) complexes and MAA-decorated CdTe

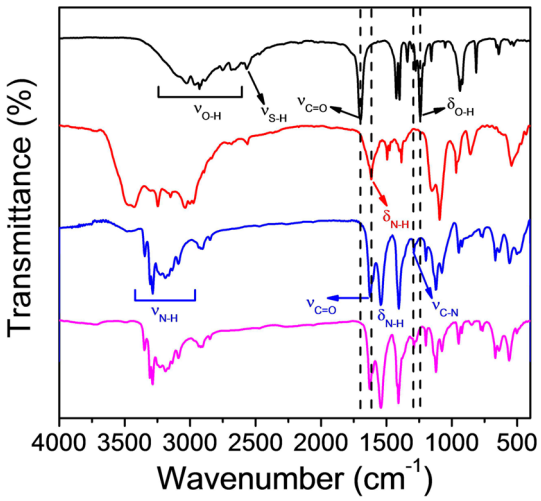

Figure 3. FTIR spectra of MPA (black), N_2H_4 (red), CdTe-free 1D structure (blue), and CdTe-contained structure (pink).

NCs in aqueous media has been demonstrated by Tang and Gao *et al.*, though the structure is not rigid.[49,57] The formation of 1D structure is essentially attributed to the electrostatic environment of aqueous media, which is commonly conducted by addition of electrolytes or water-miscible solvents.[50,58] In such environment, the interactions between nanometer-sized clusters and crystals mainly involve electrostatic repulsion, dipolar attraction, and van der Waals attraction. Electrostatic repulsion is the main driving force to keep nanoclusters stable in solution.[58] If the electrostatic repulsion is weakened, for example by adding a large amount of N_2H_4, the increased attraction will lead to aggregation/assembly of nanoclusters. Experimentally, the addition of N_2H_4 significantly lowers the zeta potential of solution, showing the decreased electrostatic repulsion (Table S2). Because dipolar attraction is anisotropic, the cooperation of various weak interactions greatly favors the self-assembly of nanoclusters with 1D orientation.[58] This means that the formation of 1D assembly structures of nanoclusters and NCs is spontaneous in aqueous media. In our experiment, the aspect ratio of 1D self-assembly materials is controlled by adjusting the equilibrium of various interactions. For example, the aspect ratio decreases with the increase of N_2H_4 concentration (Figure S6), because the significant decrease of electrostatic repulsion under high N_2H_4 concentration lowers the priority of 1D orientated assembly, while quasi-2D assembly is allowed.[58]

The rigid 1D structure is attributed to the *in situ* amidation reaction between N_2H_4 and the carboxyl of MPA at room temperature, which is proved by Fourier transform infrared (FTIR) and X-ray photoelectron spectroscopy (XPS) characterizations (Figure 3 and 4). As shown in Figure 3, the FTIR spectrum of MPA exhibits the C═O stretching vibration at 1700 cm^{-1} and S−H stretching vibration at 2566 cm^{-1}. N_2H_4 presents the N−H bending vibration at 1618 cm^{-1}.

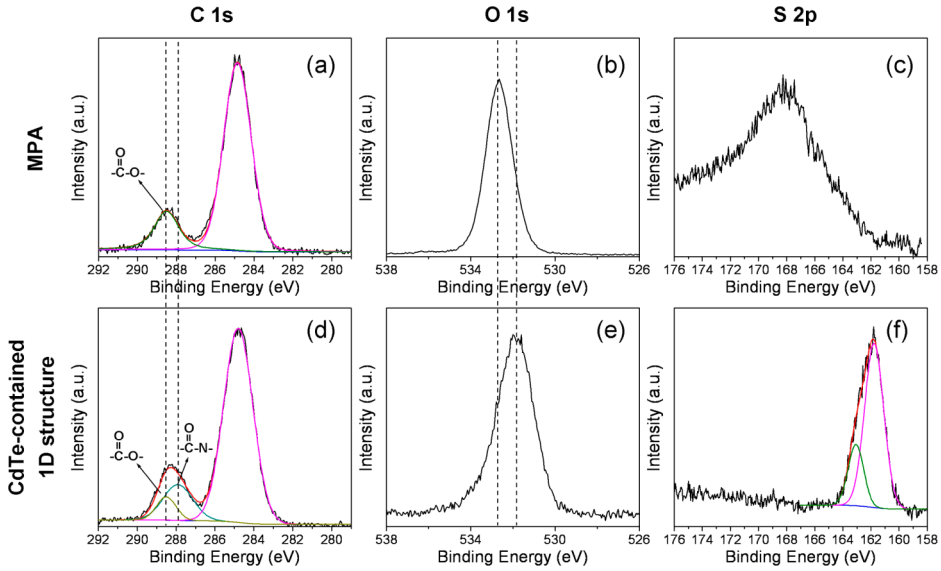

Figure 4. XPS spectra of MPA (a–c) and the as-prepared CdTe-contained 1D structure (d–f).

After forming 1D structure, the band of S–H disappears due to the formation of Cd–S bonding. Meanwhile, the C═O stretching vibration shifts to 1623 cm^{-1}, consisting with the position of amide I band. The N–H bending vibration shifts to 1542 cm^{-1}, which consists with the amide II band of secondary acyclic hydrazide. A new band appears at 1288 cm^{-1}, which is assigned to the C–N stretching vibration of hydrazide. In addition, the O–H bending vibration of MPA at 1241 cm^{-1} disappears due to the formation of hydrazide. Control experiments further exclude the existence of hydrazinium carboxylates in the 1D structure (Figure S7). Note that the needlelike 1D structures form only with high hydrazine proportion. If the mass of hydrazine is decreased, no 1D structure is found (Figure S7a).

The formation of hydrazide is also confirmed by XPS analysis of C 1s and O 1s spectra (Figure 4 and S8). Figure 4a presents the C 1s spectrum of MPA. In accordance with the structure of MPA, the C spectrum is fitted as two separated peaks at 288.5 and 284.7 eV, respectively. The former is assigned to –COOH, and the latter is assigned to $-CH_2-$.[59] In the self-assembly materials, a clear shift of –COOH peak to 287.9 eV is observed, representing the variation of —C═O chemical environment.[59] Because MPA is the only source of C, this result strongly supports the amidation of the –COOH of MPA (Figure 4d). In addition, an obvious shift of O 1s peak from 532.7 to 531.6 eV is found (Figure 4b and e). This also confirms the formation of $-CONH_2$, because the combination with N increases the electron cloud density of O and therewith decreases the binding energy.[60] Moreover, the S 2p spectrum of MPA presents a broad peak centered at 168.1 eV leading from oxidized sulfur. It means that the free MPA is easy to be oxidized in air. In contrast, the 1D structure exhibits two peaks at 161.9 and 163.2 eV, respectively, which consist well with the S $2p_{3/2}$ and S $2p_{1/2}$ peaks of normal MPA.[61] This reveals that the unstable components are protected by forming compact self-assembly materials.

To reveal the degree of cross-linkage of the self-assembly materials, the degree of amidation reaction of the –COOH groups in CdTe-free and CdTe-contained 1D structure is calculated. In CdTe-free 1D structure, MPA nearly completely reacts due to the existence of large excessive hydrazine and timely deposition of 1D structure in the solution (Figure S9). In CdTe-contained self-assembly materials, 32% –COOH on the surface of CdTe NCs are transformed into –CONH– (Figure S10). This means that CdTe NCs act as the cross-linking center to reinforce the stability of self-assembly materials, because each NC is covered by several tens of –COOH.

In all, two reasons permit to form amide bond under mild conditions, the large excessive N_2H_4 and in particular the self-separation of the products from reaction system. Because the amount of N_2H_4 is more than 1000 times to MPA, the reactive equilibrium toward hydrazide is greatly promoted. Besides, the products are insoluble in the solution, thus suppressing the reverse reaction of amidation and driving the reaction toward hydrazide.

Stability of NC Self-Assembly Materials. The NC self-assembly materials exhibit good thermal stability. Thermogravimetric analysis (TGA) data reveals that when the temperature is lower than 180 °C, no weight loss occurs for the self-assembly materials (Figure S11). The good stability is attributed to the N_2H_4-mediated cross-linkage of carboxyl-functionalized CdTe NCs, which creates a network. Note that the TGA critical temperature of NC-free 1D structure is 170 °C, slightly lower than NC-contained materials (Figure S12). This represents that NCs act as effective cross-linking centers

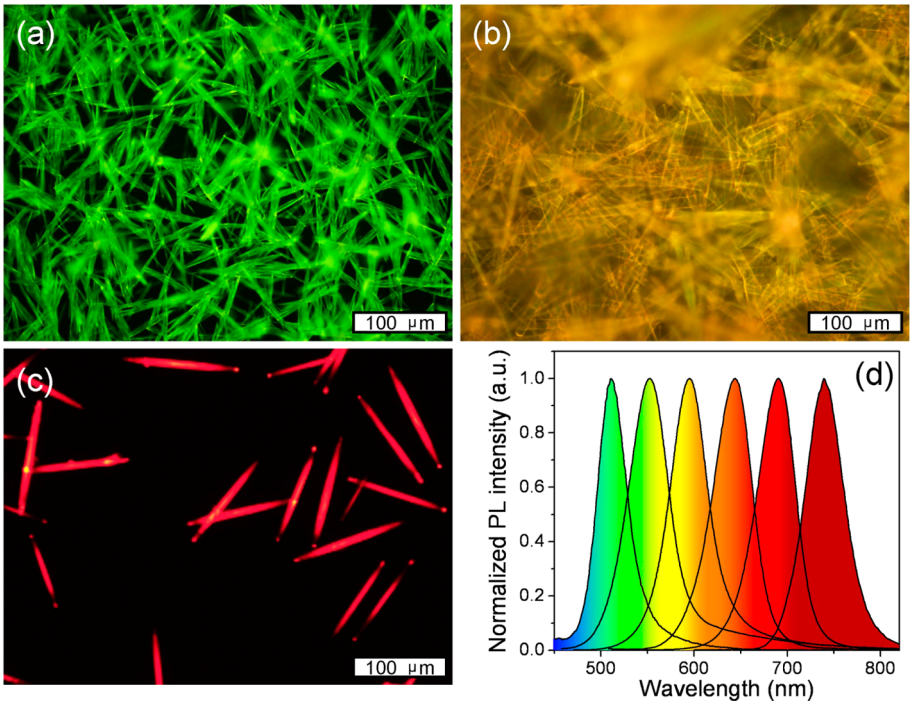

Figure 5. PL images of the self-assembly materials composed of CdTe NCs with green (a), yellow (b), and red (c) emission. (d) The emission spectra of the self-assembly materials with different emission colors.

than pure Cd-MPA complexes, thus increasing the cross-linking degree.[62] Furthermore, the low temperature resistance of NC self-assembly materials is tested in liquid nitrogen. The photoluminescence (PL) spectra of the self-assembly materials before immersing in liquid nitrogen and after returning to room temperature are compared. No PL variation is observed after such operation (Figure S13e). In contrast, the aqueous solutions of CdTe NCs frozen at −11 °C, and the melted solutions are colloidally unstable and present much lowered emission intensity (Figure S13f).

Because of the cross-linked structures, the self-assembly materials possess well solvent resistance toward hot water, alkaline solution, and organic solvents (Figure S14). As the materials are placed in 90 °C water and 1 M NaOH solution, the morphology and emission do not alter. The self-assembly materials cannot be solved or swollen by common organic solvents with different dielectric constants, such as chloroform, toluene, benzene, acetone, ethanol, dimethylformamide, and so forth. The solvent stability is comparable to highly cross-linked polymers. In contrast, both the structure and emission of uncross-linked NC self-assemblies are very fragile.

The self-assembly materials also present well resistance against sunlight and electron beam irradiation. The photostability is investigated by comparing the PL spectra of the samples with yellow emission before and after one year sunlight irradiation in air (Figure S15). No PL emission peak position and intensity variation are found for the self-assembly materials. Whereas, an obvious blue shift and intensity decrease of the PL spectra of aqueous CdTe NCs is found only after 3 days' sunlight irradiation, showing the serious photogenerated NC decomposition. In addition, the self-assembly materials keep stable upon 200 kV TEM electron beam exposure. After 30 min irradiation, no melting of 1D structure happens (Figure S16). Even the self-assembly materials are treated with 200 kV HRTEM electron beam for 10 min, the PL peak position and intensity are nearly unchanged. The dramatically high photostability is attributed to the favorable chemical surroundings. First, the self-assembly materials are cross-linked, thus isolating the NCs from the oxygen in air and suppressing the photo-oxidization under sunlight. In addition, the cross-linked network is composed of large excessive mercapto-ligands, which further protect the NCs from photo-oxidization.[63] Note that although NCs can be embedded into inorganic crystals, for example NaCl, the stability upon electron beam exposure is rather poor, because of the noncovelent linkage of NCs with the host crystals.[19] Moreover, the structural stability of self-assembly materials is evaluated by stretching self-assembly material-filled polydimethylsiloxane (PDMS), an elastic polymer matrix (Figure S17). No emission profile change is observed after stretching, because NCs are already embedded in stable self-assembly structures. In all, the excellent thermal, solvent, and photostability of current NC self-assembly materials ensure the further fabrication of photoelectric devices.

Emission Properties of NC Self-Assembly Materials. Figure 5 indicates the PL images of the self-assembly materials composed of CdTe NCs with bright emission. By tuning the size of composed NCs, the emission colors of self-

TABLE 1. Comparison of the PLQYs, the Diameter of Composed NCs, FWHM, and Emission Lifetimes of Self-Assembly Materials and Unassembled CdTe NCs

PL peak position (nm)		510	560	600	640	680	750
diameter of CdTe NCs (nm)		2.2	2.6	3.1	3.6	4.1	5.2
PLQYs of self-assembly materials (%)		26	72	61	60	55	52
fwhm (nm)		38	49	47	49	48	49
emission lifetime[a]	τ_1	4.9	5.9	6.4	7.3	9.4	9.8
	τ_2	23.8	27.5	29.6	33.6	35.5	42.1
PLQYs of aqueous CdTe NCs (%)		7	15	7	2	—[b]	—[b]
fwhm (nm)		37	59	90	112	—[b]	—[b]
emission lifetime[a]	τ_1	4.9	6.9	6.6	6.1	—[b]	—[b]
	τ_2	23.6	26.9	27.1	29.6	—[b]	—[b]

[a] The PL decay curve for each sample has a biexponential form of $A_1\exp(-t/\tau_2) + A_2\exp(-t/\tau_2)$, where two lifetime components (τ_1 and τ_2) are obtained through properly fitting. [b] The CdTe NCs with emission centered at 680 and 750 nm are hardly synthesized through conventional refluxing method. Overall, when the emission center of CdTe NCs is larger than 660 nm, the NCs will be unstable and possess two emission peaks.

assembly materials are tunable from 510 to 750 nm, covering the color range from green to red (Figure 5d and Table 1). The self-assembly materials show enhanced photoluminescence quantum yields (PLQYs) up to 72% (Table 1), which is close to that of commercial yttrium aluminum garnetphosphors with yellow emission. In contrast, the conventional NC-contained nanocomposites usually exhibit decreased QYs (Table 1).[64] In the conventional procedure of fabricating nanocomposites, postpreparation treatment is applied to improve the compatibility of NCs with the composites. The loss of NC surface atoms and/or ligand removal cannot be avoided, thus increasing surface dangling bonds.[65] This suppresses the pathway of exciton radiative transition and lowers the PLQYs. In contrast, the framework of the self-assembly materials is composed of large excessive Cd and MPA, which are necessary components to passivate NCs by saturating the surface dangling bonds. This greatly favors radiative transition. So, the PLQYs are reasonably enhanced. As shown in Table 1, the emission lifetimes of self-assembly materials are generally longer than those of bare NCs, implying the improved emission properties of the NCs in the self-assembly materials.[66,67] In addition, concentration quenching is another reason for the lowered PLQYs of luminescent nanocomposites, because of the phase separation of NCs.[64] The current route effectively avoids phase separation and subsequent concentration quenching by generating a well distribution of NCs in the self-assembly materials (Figure 1e). As a result, the PLQYs of self-assembly materials are more than four times higher than the composed NCs with the same size (Table 1). Moreover, the concentration of NCs in the self-assembly materials is high, so FRET and PL reabsorption are inevitable. However, the PL loss is compensated by the PL enhancement from the favorable chemical surrounding.[68] Although the self-assembly materials possess 1D structures, neither polarized emission nor excitation polarization-dependent emission is observed (Figure S18). This is attributed to the disordered array of NCs in the self-assembled structures.

The full width at half-maximum (fwhm) of the PL spectra of self-assembly materials is also narrow (Table 1). Even for the samples with the emission peak at 750 nm, the fwhm is only 49 nm, which are narrower among the luminescent materials. For example, the fwhm of commercial yttrium aluminum garnetphosphors is *ca.* 100 nm.[16] The narrow PL spectra are resulted both from the hydrazine-promoted NC synthesis and the reabsorption of short wavelength part of NC PL in the self-assembly materials. As revealed in our previous work,[51] hydrazine-promoted NC synthesis avoids the decomposition of mercapto-ligands and hence the embedment of S into CdTe NCs. Consequently, the PL peak is narrower than that of the NCs prepared through conventional reflux at 100 °C (Table 1). In addition, because the concentration of NCs in the self-assembly materials is much high, the reabsorption of short wavelength part of the PL is inevitable. So, the PL spectrum of NC ensemble is further narrowed. The narrow PL spectra mean high color purity, which is necessary for precise design of LEDs.

Because of the high performance of NC self-assembly materials, they are employed as the color conversion layer to fabricate a LED prototype. After mixing the self-assembly materials and PDMS precursor solutions with specific ratio, the mixtures are deposited on commercially available 0.2 W InGaN LED chip, and cured in an oven at 100 °C for 2 h. The LED devices with green, yellow, and red emissions are obtained using the self-assembly materials with corresponding emission color (Figure 6a−c). Because of the high PLQYs, only 1 wt % self-assembly materials is required in the PDMS. In addition, the RGB color coordinates of the LED are (0.68, 0.31), (0.19, 0.75), (0.14, 0.04) (Figure 6d). The area of the RGB triangle of the LED covers most of the NTSC color space (104.3%). In contrast, the phosphor-LED covers only 85.6% according to the previous report.[17] A simple WLED with color coordinate (x, y) = (0.31, 0.31) is fabricated by integrating the 450 nm blue emission of InGaN chip and 557 nm yellow emission of NC self-assembly materials (Figure S19). Despite the bright white emission, the LED indicates a low CRI below 50. It is known that sunlight possesses the highest CRI of 100. To fabricate WLEDs with high CRI, further optimization of self-assembly materials is still required.

Control of NC Concentration and Component in Self-Assembly Materials. To design the NC-based LEDs highly similar to sunlight, it requires further control of emission color and intensity of self-assembly materials. Although bright and color-tunable emissions are achieved through the aforementioned one pot route, it is less capable to control NC concentration in the self-assembly materials. In addition, besides CdTe, the one pot route cannot

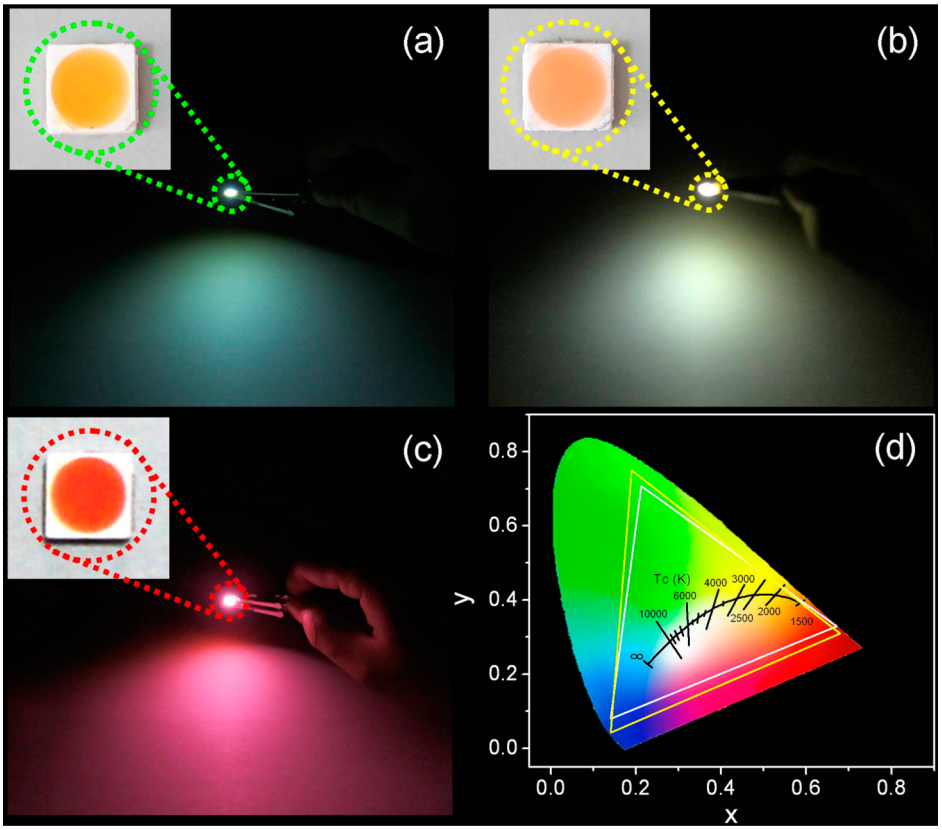

Figure 6. LED prototypes with green (a), yellow (b), and red (c) emission. Insets in (a−c) are the photographs of LED taken at sunlight. (d) Color triangles of LED (yellow) compared to NTSC1931 (white), the black curve represents the variation of color temperature with the color coordinates, and the points on the black straight line are constant color temperature.

produce the self-assembly materials from other NCs. To solvent the problems, an alternative route to produce NC self-assembly materials is proposed on the basis of N_2H_4-midiated cross-linkage of Cd-MPA complexes. In this method, N_2H_4 are foremost added into the aqueous solutions of $CdCl_2$ and MPA to induce the 1D structure of Cd-MPA complexes. Just before the appearance of NC-free 1D structure, additional NCs are added to produce NC-contained self-assembly materials. The emission color, volume, and/or concentration of additional NC solutions can be randomly adjusted (Table S3), thus permitting to control the emission properties of the self-assembly materials in broad range. This method is extendable to other NCs, such as MPA-modified CdS, CdSe, $CdSe_xTe_{1-x}$, and $Cd_yHg_{1-y}Te$ NCs (Figure S20). Moreover, other mercapto carboxylic acids, such as MAA, thiolactic acid (TLA), and mercaptosuccinic acid (MSA), are also adopted as the capping ligands to prepare 1D self-assembly materials. However, only MAA is workable due to the similar straight chain structure with MPA (Figure S21). The uselessness of TLA and MSA is attributed to the steric hindrance from the side chain, which prevents the formation of self-assembly materials with regular crystalline structure (Figure 2b). The current method is not limited to aqueous synthesized NCs. The NCs originally synthesized in organic media, for example CdSe NCs, can also form 1D self-assembly materials after surface ligand exchange using MPA (Figure S22). These reveals the universality of current N_2H_4-midiated construction of NC self-assembly materials.

Besides N_2H_4, other short diamine, for example ethylenediamine ($NH_2CH_2CH_2NH_2$), is also tested. However, self-assembly materials can not form. This is attributed to the following reasons. First, $NH_2CH_2CH_2NH_2$ possesses two more methylene in comparison with hydrazine. The high steric hindrance prevents the formation of self-assembly materials with regular structure. Second, the stability constant of Cd-$NH_2CH_2CH_2NH_2$ is several orders larger than that of Cd-NH_2NH_2 (log $K_{Cd\text{-}NH_2CH_2CH_2NH_2} = 5.47$, log $K_{Cd\text{-}NH_2NH_2} = 2.25$). The strong coordination between Cd and $NH_2CH_2CH_2NH_2$ leads to the decomposition of CdTe NCs.[69] Third, in comparison to hydrazine, $NH_2CH_2CH_2NH_2$ possesses lower reactivity in forming amide.[70] So, the production of NC self-assembly materials at room temperature are not successful as replacing hydrazine with other short diamine. Note that although hydrazine is toxic, the form of hydrazine in the final materials is hydrazide. The toxicity is much lower than free hydrazine. In addition, the hydrazine remained in the solution can be easily recycled and reused, owing to the self-separation of the products from the growth solution.[51] Because of the high stability of the materials, the toxicity of embedded Cd-contained NCs is also lowered.

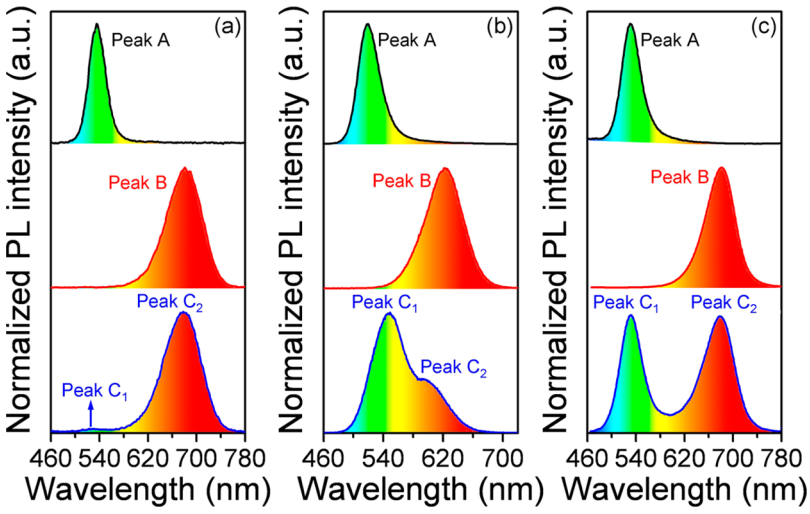

Figure 7. (a) The PL spectra of aqueous CdTe NCs with emission at 535 nm (black), 682 nm (red), and their mixture (blue). (b) The PL spectra of aqueous CdTe NCs with emission at 535 nm (black), 642 nm (red), and their mixture (blue) in the presence of N_2H_4. (c) The PL spectra of self-assembly materials with emission at 530 nm (black), 682 nm (red), and their mixture (blue).

WLEDs from Self-Assembly Materials. An ideal method to fabricate NC-based high performance WLEDs is the direct blending of different emitted NCs with specific ratio. The WLED has been tried by proportional mixing the aqueous NC components with different emission colors. However, the practical operation meets several problems. First, NC components with different emission colors show tremendous difference in their PLQYs, making it very difficult to tune the final emission by adjusting the feed ratio. Second, when the aqueous solutions of different sized NCs are mixed, the FRET from smaller NCs to larger ones increases the red emission part by serious weakening green part in the NC ensembles (Figure 7a). Although FRET is avoidable by lowering NC concentration to enlarge the distance in between NCs (Figure S23), the overall PL intensity is too weak for LED applications. These reasons lead to the uncertainty in emission control. Consequently, the fabrication of NC-based LED with high CRI from unassembled aqueous NCs is practically impossible. We attempt to prepare the self-assembly materials containing different sized CdTe NCs. However, due to the promotion of N_2H_4 in NC size evolution, the intermediately sized NCs are generated *via* a spontaneous inter-NC size ripening process (Figure 7b).[71] Consequently, the self-assembly materials with single emission colors are employed to fabricate WLEDs.

The capability to control the emission properties of NC self-assembly materials allows to fabricate WLEDs by direct blending route. Importantly, both the FRET and PL reabsorption are limited inner the self-assembly materials, because the NCs are already preassembled. As the self-assembly materials with different emission colors are blended in fabricating WLED, no PL quenching and spectral shift is observed (Figure 7c). This is one of the advantages of the current method. This finding greatly facilitates the design of WLEDs with high CRI by unifying the real emission and the calculated material ratio. As shown in Figure 8a–c, a WLED with the CRI of 86 is fabricated by integrating the emissions of InGaN chip and six NC self-assembly materials. The emission peaks of self-assembly materials are centered at 520, 560, 590, 631, 680, and 750 nm. The feed ratio is 3/1/0.8/0.5/0.5/0.5. The spectrum of WLED is much similar to sunlight (Figure 8b and g). To examine the color rendering property of WLED, the different colored pen caps with high color saturation are illuminated by the WLED and sunlight for a comparison (Figure 8a and f). The apparent colors are nearly identical, showing the good color rendering property of WLED. In CRI calculation, eight pastel test color samples (TCS01–08, Figure 8e), which are mediate color saturation, are used to compare the color rendering properties of the light in question with a reference light source in colorimetry.[72] Six additional colors (TCS09–14) are also indicated to emphasize the good color rendering properties, but they are not used for calculating CRI (Figure 8e). To eliminate local overexposure originated from point light source, an area light, composed of nine WLED devices, are fabricated for testing the color rendering property (Figure 8d and S24). As shown in Figure 8e, the color of TCS01–14 is well displayed in comparison with the original electronic version (Figure S25). All the above measurements prove that the WLED possesses good color rendering property. Moreover, the efficacy of the WLED is 37 lm/W at the coordinate $(x, y) = (0.32, 0.33)$ and color temperature of 6110 K. The turn-on voltage is 2.5 V. The intensity of LED is strong enough to illuminate an A4 paper under the operation voltage of 3.0 V (Figure 8a). In addition, according to the theory of colorimetry, the LED with any emission colors in the triangle can be obtained by mixing the self-assembly materials with different emission colors (Figure 6d). The black curve represents the

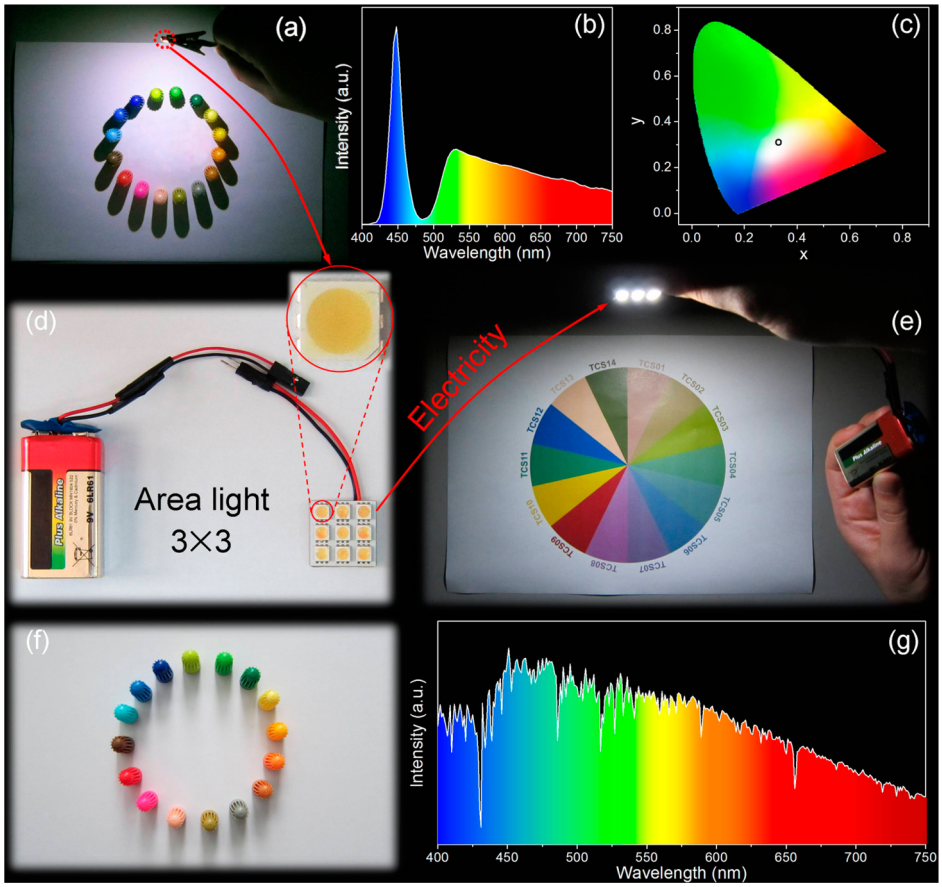

Figure 8. (a) An A4 paper is illuminated by a single WLED device. Different colored pen caps and printed letters are used for testing the CRI. Corresponding emission spectrum (b), and color coordinate (c) of WLED are also shown. (d) An area light composed of nine WLED devices. (e) An A4 paper with different color picture is printed. TCS: test color samples for calculating CRI. (f) The same A4 paper in (a) is illuminated by sunlight. (g) The emission spectrum of sunlight. For the fabrication of WLED, six NC self-assembly materials with different emission colors are foremost prepared by one-pot route.

variation of color temperature with the color coordinates, and the points on the black straight line are constant color temperature (Figure 6d). It reveals that the color temperature of LED is tuned from 1500 to tens of thousands degrees Kelvin, covering all color temperatures from the poles to the equator. To prove this, three WLEDs with different color temperatures are fabricated, and the characteristics are listed (Figure S26). Finally, the WLED is tested at different operation voltage. The decreased voltage only lowers the brightness, but not alters the emission color and CRI (Figure S27).

CONCLUSIONS

In summary, 1D self-assembly materials from aqueous luminescent NCs are facilely fabricated by integrating the NC synthesis, spontaneous assembly, and *in situ* polymerization completely in one pot. The key is the additive N_2H_4, which simultaneously promotes the room-temperature synthesis of NCs, induces the 1D orientated self-assembly of NCs, and participate the polymerization with mercapto carboxylic acid-modified NCs *via in situ* amidation reaction. The amidation of the carboxyls on NC surface makes the NCs as macromonomers to form cross-linked self-assembly materials. In comparison with the previous NC self-assembly structures, the current self-assembly materials exhibit excellent stability, high PLQYs, tunable compositions and emission color. In particular, FRET between different emitting NCs is avoided, thus overcoming the main problem in design WLED from multiple NC components. These advantages permit to fabricate the WLED from NC self-assembly materials with high luminous efficacy, high CRI, and tunable color temperature. For the best representative WLED, the CRI, color temperature, and luminous efficacy is 86, 6110 K, and 37 lm/W, respectively.

METHODS

Materials. Tellurium powder (~200 mesh, 99.8%), selenium powder (−100 mesh, 99.5+ %), 3-mercaptopropionic acid (MPA, 99+ %), mercaptoacetic acid (MAA, 98%), and 2-mercaptoethylamine (MA, 98%) were purchased from Aldrich. $NaBH_4$ (96%), $Na_2S \cdot 9H_2O$ (98+%), Na_2TeO_3 (98+%), $CdCl_2$ (99%),

$HgCl_2$ (99%), thiolactic acid (TLA, 99+%), mercaptosuccinic acid (MSA, 99+%), 2-propanol (99%), and $N_2H_4 \cdot H_2O$ (80%) were commercially available products and used as received. Polydimethylsiloxane (PDMS) elastomer kits (Sylgard 184) were purchased from Dow Corning (Midland, MI).

Room-Temperature One-Pot Preparation of CdTe NC Self-Assembly Materials in the Presence of N_2H_4. The preparation combined the synthesis, preassembly, and *in situ* polymerization of aqueous CdTe NCs completely in one pot. Typically, 8 mL of 100 mM $CdCl_2$ aqueous solution, 64 mL of water, 142 μL of MPA, 8 mL of 20 mM Na_2TeO_3 aqueous solution, and 100 mg of $NaBH_4$ were added in a conical flask in turn. The concentration of precursors was 10 mM referring to Cd^{2+}, and the molar ratio of Cd^{2+}/MPA/TeO_3^{2-}/$NaBH_4$ was 1:2.0:0.2:3.4. After maintaining the precursors in the dark at room temperature for 48 h, 80 mL of 80% $N_2H_4 \cdot H_2O$ was added. Sixteen hours later, CdTe NC self-assembly materials were observed at the bottom of the flask. By altering precursor and/or N_2H_4 concentration, the emission peaks of self-assembly materials were tunable from 510 to 750 nm, which corresponded to the emission colors from green to red.

Preparation of Mercapto Carboxylic Acid-Modified Aqueous CdS, CdSe, CdTe, $CdSe_xTe_{1-x}$, and $Cd_yHg_{1-y}Te$ NCs in the Absence of N_2H_4. Typically, MPA-modified CdTe precursors were prepared by injecting freshly prepared NaHTe aqueous solution into N_2-saturated $CdCl_2$ solution at pH 9.5 in the presence of MPA.[54] The concentration of precursors was 10 mM referring to Cd^{2+}, and the molar ratio of Cd^{2+}/MPA/HTe^- was 1:2.0:0.2. The precursor solutions were refluxed at 100 °C to maintain NC growth. Aliquots of the refluxed solutions were taken after different time intervals to obtain the NCs with different emission colors. For further characterization, the NC solutions were purified by centrifugation with the addition of 2-propanol. Following a similar procedure, except using Na_2S, NaHSe, or $NaHSe_xTe_{1-x}$ as the chalcogenide sources, CdS, CdSe, and $CdSe_xTe_{1-x}$ NCs were prepared. $Cd_yHg_{1-y}Te$ NCs were prepared using $CdCl_2$/$HgCl_2$ mixed solutions as the metal sources with other experimental parameters similar to CdTe synthesis. Other mercapto carboxylic acids, such as MAA, TLA, and MSA are also available for the aforementioned NC synthesis.

Self-Assembly Structures of Cd-MPA Complexes in the Presence of N_2H_4. N_2H_4-mediated self-assembly and cross-linkage of Cd-MPA complexes were achieved by mixing 8 mL of 100 mM $CdCl_2$ aqueous solution, 72 mL of water, 106 μL of MPA, and 80 mL of 80% N_2H_4 in a breaker at room temperature. The calculated molar ratio of Cd^{2+}/MPA/N_2H_4 was 1:1.5:1650. Two hours later, the self-assembly structures were observed at the bottom of the beaker.

Surface Modification of the CdSe NCs Synthesized in Organic Media. CdSe NCs were synthesized in high-boiling-point organic solvents according to the previous publication.[73] MPA was modified on CdSe NCs *via* ligand exchange, which transferred the NCs from organic media to water.[74]

Self-Assembly Materials *via* Supplement of As-Synthesized NCs into Cd-MPA Complexes. In this route, the production of NC self-assembly materials is based on the preparation of Cd- MPA self-assembly structures with slight modification. After adding N_2H_4 into the mixture of $CdCl_2$ and MPA, the NC solutions, such as CdS, CdSe, CdTe, $CdSe_xTe_{1-x}$ and $Cd_yHg_{1-y}Te$, with specific concentration, volume, and emission color were added. Two hours later, the self-assembly materials with specific NC component, concentration, and emission color were produced.

Fabrication of LEDs from NC Self-Assembly Materials. InGaN LED chips without phosphor coating were purchased from Shen Zhen Hongcai Elecronics CO., Ltd. The microchip was attached on the bottom of the LED base. The emission of the LED chip was centered at 450 nm, and the operating voltage was 3.0 V. The two leads on LED were prepared to connect to the power supply. In the preparation of color conversion layer, NC self-assembly materials with different emission colors were foremost mixed with specific ratio and milled to fine powder. Then, the PDMS precursors were mixed with the powder with the ratio of 18:1 (w/w). The mixtures were put in a vacuum chamber to remove bubbles. After that, the mixtures were filled into the cup-shaped void of LED chip. After curing at 100 °C for 2 h, the LEDs from NC self-assembly materials were fabricated.

Characterization. UV−visible absorption spectra were obtained using a Lambda 800 UV−vis spectrophotometer. Photoluminescent (PL) spectroscopy was performed with a Shimadzu RF-5301 PC spectrophotometer. The excitation wavelength was 400 nm. The PLQYs of NCs were estimated at room temperature using quinine in 0.5 mol/L H_2SO_4 aqueous solution as the PL reference.[71] Transmission electron microscopy (TEM) was conducted using a Hitachi H-800 electron microscope at an acceleration voltage of 200 kV with a CCD camera. High-resolution TEM (HRTEM) imaging was implemented by a JEM-2100F electron microscope at 200 kV. Scanning electron microscope (SEM) image was taken with a JEOL FESEM 6700F electron microscope with primary electron energy of 3 kV. Energy dispersive spectrum (EDS) and mapping were conducted with Inca X-Max instruments made by Oxford Instruments. An Olympus BX-51 fluorescence microscope with a CCD camera was used to examine the photoluminescent self-assembly materials. Thermogravimetric analysis (TGA) was measured on an American TA Q500 analyzer under N_2 atmosphere with the flow rate of 100 mL·min^{-1}. Fourier transform infrared (FTIR) spectra were performed with a Nicolet AVATAR 360 FTIR instrument. X-ray photoelectron spectroscopy (XPS) was investigated using a VG ESCALAB MKII spectrometer with a Mg KR excitation (1253.6 eV). Binding energy calibration was based on C 1s at 284.6 eV. Inductive coupled plasma emission spectrometer (ICP) was carried out with PERKIN ELMER OPTIMA 3300DV analyzer. X-ray powder diffraction (XRD) investigation was carried out using Siemens D5005 diffractometer. The color of light was identified by the CIE (Commission Internationale de L'Eclairage 1931) colorimetry system. Any color could be described by the chromaticity (x, y) coordinates on the CIE diagram. The absolute PLQYs of CdTe-contained 1D structure were measured on Edinburgh FLS920 (excited at 400 nm) equipped with an integrating sphere. Before the measurement, the instrument was calibrated by the quinine in 0.5 mol/L H_2SO_4 aqueous solution, where the final concentration was 1×10^{-5} mol/L to eliminate the concentration quenching. The measured PLQY of quinine was demonstrated to be equal to the real one. Then, the blank laser excitation line of 400 nm was measured first. Then, the sample was placed on the sample holder in the integrating sphere for the measurements of the emission spectra. Finally, the QYs were calculated according to the previous paper, with the software supplied by the manufacturer.[75] The spectra and brightness−current density−voltage characteristics of the LED were measured by combining a Spectrascan PR-650 spectrophotometer with an integral sphere and a computer-controlled direct-current power supply Keithley model 2400 voltage−current source under ambient condition at room temperature.

Conflict of Interest: The authors declare no competing financial interest.

Acknowledgment. This work was supported by the 973 Program of China (2014CB643503), NSFC (51425301, 21374042, 21174051, 91123031, 51433003, 21221063), and the Special Project from MOST of China.

Supporting Information Available: The preparation procedure of NC self-assembly materials, the characterization of CdTe-free 1D structure, the calculations of amidation degree, the stabilities of self-assembly materials, and the additional information on LEDs. This material is available free of charge *via* the Internet at http://pubs.acs.org.

REFERENCES AND NOTES

1. Tang, Z. Y.; Zhang, Z. L.; Wang, Y.; Glotzer, S. C.; Kotov, N. A. Self-Assembly of CdTe Nanocrystals into Free-Floating Sheets. *Science* **2006**, *314*, 274–278.
2. Mokari, T.; Rothenberg, E.; Popov, I.; Costi, R.; Banin, U. Selective Growth of Metal Tips onto Semiconductor Quantum Rods and Tetrapods. *Science* **2004**, *304*, 1787–1790.
3. Peng, X. G.; Manna, L.; Yang, W. D.; Wickham, J.; Scher, E.; Kadavanich, A.; Alivisatos, A. P. Shape Control of CdSe Nanocrystals. *Nature* **2000**, *404*, 59–61.

4. Murray, C. B.; Kagan, C. R.; Bawendi, M. G. Self-Organization of CdSe Nanocrystallites into Three-Dimensional Quantum Dot Superlattices. *Science* **1995**, *270*, 1335–1338.
5. Xia, Y. S.; Nguyen, T. D.; Yang, M.; Lee, B.; Santos, A.; Podsiadlo, P.; Tang, Z. Y.; Glotzer, S. C.; Kotov, N. A. Self-Assembly of Self-Limiting Monodisperse Supraparticles from Polydisperse Nanoparticles. *Nat. Nanotechnol.* **2011**, *6*, 580–587.
6. Konstantatos, G.; Howard, I.; Fischer, A.; Hoogland, S.; Clifford, J.; Klem, E.; Levina, L.; Sargent, E. H. Ultrasensitive Solution-Cast Quantum Dot Photodetectors. *Nature* **2006**, *442*, 180–183.
7. McDonald, S. A.; Konstantatos, G.; Zhang, S. G.; Cyr, P. W.; Klem, E. J. D.; Levina, L.; Sargent, E. H. Solution-Processed PbS Quantum Dot Infrared Photodetectors and Photovoltaics. *Nat. Mater.* **2005**, *4*, 138–142.
8. Daniel, M. C.; Astruc, D. Gold Nanoparticles: Assembly, Supramolecular Chemistry, Quantum-Size-Related Properties, and Applications toward Biology, Catalysis, and Nanotechnology. *Chem. Rev.* **2004**, *104*, 293–346.
9. Whaley, S. R.; English, D. S.; Hu, E. L.; Barbara, P. F.; Belcher, A. M. Selection of Peptides with Semiconductor Binding Specificity for Directed Nanocrystal Assembly. *Nature* **2000**, *405*, 665–668.
10. Han, M. Y.; Gao, X. H.; Su, J. Z.; Nie, S. H. Quantum-Dot-Tagged Microbeads for Multiplexed Optical Coding of Biomolecules. *Nat. Biotechnol.* **2001**, *19*, 631–635.
11. Medintz, I. L.; Uyeda, H. T.; Goldman, E. R.; Mattoussi, H. Quantum Dot Bioconjugates for Imaging, Labelling and Sensing. *Nat. Mater.* **2005**, *4*, 435–446.
12. Jr, B. M.; Moronne, M.; Gin, P.; Weiss, S.; Alivisatos, A. P. Semiconductor Nanocrystals as Fluorescent Biological Labels. *Science* **1998**, *281*, 2013–2016.
13. Dubertret, B.; Skourides, P.; Norris, D. J.; Noireaux, V.; Brivanlou, A. H.; Libchaber, A. *In Vivo* Imaging of Quantum Dots Encapsulated in Phospholipid Micelles. *Science* **2002**, *298*, 1759–1762.
14. Lin, Y.; Skaff, H.; Emrick, T.; Dinsmore, A. D.; Russell, T. P. Nanoparticle Assembly and Transport at Liquid-Liquid Interfaces. *Science* **2003**, *299*, 226–229.
15. Gaponik, N.; Wolf, A.; Marx, R.; Lesnyak, V.; Schilling, K.; Eychmüller, A. Three-Dimensional Self-Assembly of Thiol-Capped CdTe Nanocrystals: Gels and Aerogels as Building Blocks for Nanotechnology. *Adv. Mater.* **2008**, *20*, 4257–4262.
16. Kim, S.; Kim, T.; Kang, M.; Kwak, S. K.; Yoo, T. W.; Park, L. S.; Yang, I.; Hwang, S.; Lee, J. E.; Kim, S. K.; *et al.* Highly Luminescent InP/GaP/ZnS Nanocrystals and Their Application to White Light-Emitting Diodes. *J. Am. Chem. Soc.* **2012**, *134*, 3804–3809.
17. Jang, E.; Jun, S.; Jang, H.; Lim, J.; Kim, B.; Kim, Y. White-Light-Emitting Diodes with Quantum Dot Color Converters for Display Backlights. *Adv. Mater.* **2010**, *22*, 3076–3080.
18. Kim, K.; Woo, J. Y.; Jeong, S.; Han, C. S. Photoenhancement of a Quantum Dot Nanocomposite *via* UV Annealing and Its Application to White LEDs. *Adv. Mater.* **2011**, *23*, 911–914.
19. Otto, T.; Müller, M.; Mundra, P.; Lesnyak, V.; Demir, H. V.; Gaponik, N.; Eychmüller, A. Colloidal Nanocrystals Embedded in Macrocrystals: Robustness, Photostability, and Color Purity. *Nano Lett.* **2012**, *12*, 5348–5354.
20. Jun, S.; Lee, J.; Jang, E. Highly Luminescent and Photostable Quantum Dot-Silica Monolith and Its Application to Light-Emitting Diodes. *ACS Nano* **2013**, *7*, 1472–1477.
21. Dai, Q.; Duty, C. E.; Hu, M. Z. Semiconductor-Nanocrystals-Based White Light-Emitting Diodes. *Small* **2010**, *6*, 1577–1588.
22. Rogach, A. L.; Gaponik, N.; Lupton, J. M.; Bertoni, C.; Gallardo, D. E.; Dunn, S.; Li Pira, N.; Paderi, M.; Repetto, P.; Romanov, S. G.; *et al.* Light-Emitting Diodes with Semiconductor Nanocrystals. *Angew. Chem., Int. Ed.* **2008**, *47*, 6538–6549.
23. Murray, C. B.; Norris, D. J.; Bawendi, M. G. Synthesis and Characterization of Nearly Monodisperse CdE (E = S, Se, Te) Semiconductor Nanocrystallites. *J. Am. Chem. Soc.* **1993**, *115*, 8706–8715.
24. Rajh, T.; Mićić, O. I.; Nozik, A. J. Synthesis and Characterization of Surface-Modified Colloidal CdTe Quantum Dots. *J. Phys. Chem.* **1993**, *97*, 11999–12003.
25. Cao, Y. W.; Banin, U. Growth and Properties of Semiconductor Core/Shell Nanocrystals with InAs Cores. *J. Am. Chem. Soc.* **2000**, *122*, 9692–9702.
26. Gaponik, N.; Talapin, D. V.; Rogach, A. L.; Hoppe, K.; Shevchenko, E. V.; Kornowski, A.; Eychmüller, A.; Weller, H. Thiol-Capping of CdTe Nanocrystals: An Alternative to Organometallic Synthetic Routes. *J. Phys. Chem. B* **2002**, *106*, 7177–7185.
27. Tang, K. B.; Qian, Y. T.; Zeng, J. H.; Yang, X. G. Solvothermal Route to Semiconductor Nanowires. *Adv. Mater.* **2003**, *15*, 448–450.
28. Nedeljković, J. M.; Mićić, O. I.; Ahrenkiel, S. P.; Miedaner, A.; Nozik, A. J. Growth of InP Nanostructures *via* Reaction of Indium Droplets with Phosphide Ions: Synthesis of InP Quantum Rods and InP-TiO_2 Composites. *J. Am. Chem. Soc.* **2004**, *126*, 2632–2639.
29. Pang, Q.; Zhao, L. J.; Cai, Y.; Nguyen, D. P.; Regnault, N.; Wang, N.; Yang, S. H.; Ge, W. K.; Ferreira, R.; Bastard, G.; *et al.* CdSe Nano-Tetrapods: Controllable Synthesis, Structure Analysis, and Electronic and Optical Properties. *Chem. Mater.* **2005**, *17*, 5263–5267.
30. Qian, H. F.; Dong, C. Q.; Weng, J. F.; Ren, J. C. Facile One-Pot Synthesis of Luminescent, Water-Soluble, and Biocompatible Glutathione-Coated CdTe Nanocrystals. *Small* **2006**, *2*, 747–751.
31. Green, M.; Harwood, H.; Barrowman, C.; Rahman, P.; Eggeman, A.; Festry, F.; Dobson, P.; Ng, T. A Facile Route to CdTe Nanoparticles and Their Use in Bio-Labelling. *J. Mater. Chem.* **2007**, *17*, 1989–1994.
32. He, Y.; Sai, L. M.; Lu, H. T.; Hu, M.; Lai, W. Y.; Fan, Q. L.; Wang, L. H.; Huang, W. Microwave-Assisted Synthesis of Water-Dispersed CdTe Nanocrystals with High Luminescent Efficiency and Narrow Size Distribution. *Chem. Mater.* **2007**, *19*, 359–365.
33. Sgobba, V.; Schulz-Drost, C.; Guldi, D. M. Synthesis and Characterization of Positively Capped CdTe Quantum Wires That Exhibit Strong Luminescence in Aqueous Media. *Chem. Commun.* **2007**, 565–567.
34. Zheng, Y. G.; Gao, S. J.; Ying, J. Y. Synthesis and Cell-Imaging Applications of Glutathione-Capped CdTe Quantum Dots. *Adv. Mater.* **2007**, *19*, 376–380.
35. Ouyang, J. Y.; Zaman, M. B.; Yan, F. J.; Johnston, D.; Li, G.; Wu, X. H.; Leek, D.; Ratcliffe, C. I.; Ripmeester, J. A.; Yu, K. Multiple Families of Magic-Sized CdSe Nanocrystals with Strong Bandgap Photoluminescence *via* Noninjection One-Pot Syntheses. *J. Phys. Chem. C* **2008**, *112*, 13805–13811.
36. Zou, L.; Gu, Z. Y.; Zhang, N.; Zhang, Y. L.; Fang, Z.; Zhu, W. H.; Zhong, X. H. Ultrafast Synthesis of Highly Luminescent Green- to Near Infrared-Emitting CdTe Nanocrystals in Aqueous Phase. *J. Mater. Chem.* **2008**, *18*, 2807–2815.
37. Xia, Y. S.; Tang, Z. Y. Monodisperse Hollow Supraparticles *via* Selective Oxidation. *Adv. Funct. Mater.* **2012**, *22*, 2585–2593.
38. Mamedov, A. A.; Belov, A.; Giersig, M.; Mamedova, N. N.; Kotov, N. A. Nanorainbows: Graded Semiconductor Films from Quantum Dots. *J. Am. Chem. Soc.* **2001**, *123*, 7738–7739.
39. Guo, J.; Yang, W. L.; Wang, C. C. Systematic Study of the Photoluminescence Dependence of Thiol-Capped CdTe Nanocrystals on the Reaction Conditions. *J. Phys. Chem. B* **2005**, *109*, 17467–17473.
40. Shieh, F.; Saunders, A. E.; Korgel, B. A. General Shape Control of Colloidal CdS, CdSe, CdTe Quantum Rods and Quantum Rod Heterostructures. *J. Phys. Chem. B* **2005**, *109*, 8538–8542.
41. Wang, X.; Zhuang, J.; Peng, Q.; Li, Y. D. A General Strategy for Nanocrystal Synthesis. *Nature* **2005**, *437*, 121–124.
42. Warner, J. H.; Tilley, R. D. Synthesis and Self-Assembly of Triangular and Hexagonal CdS Nanocrystals. *Adv. Mater.* **2005**, *17*, 2997–3001.
43. Bao, H. F.; Wang, E. K.; Dong, S. J. One-Pot Synthesis of CdTe Nanocrystals and Shape Control of Luminescent CdTe-Cystine Nanocomposites. *Small* **2006**, *2*, 476–480.

44. Ludolph, B.; Malik, M. A.; O'Brien, P.; Revaprasadu, N. Novel Single Molecule Precursor Routes for the Direct Synthesis of Highly Monodispersed Quantum Dots of Cadmium or Zinc Sulfide or Selenide. *Chem. Commun.* **1998**, 1849–1850.
45. Steckel, J. S.; Snee, P.; Coe-Sullivan, S.; Zimmer, J. P.; Halpert, J. E.; Anikeeva, P.; Kim, L. A.; Bulovic, V.; Bawendi, M. G. Color-Saturated Green-Emitting QD-LEDs. *Angew. Chem., Int. Ed.* **2006**, *45*, 5796–5799.
46. Xie, R. G.; Kolb, U.; Basché, T. Design and Synthesis of Colloidal Nanocrystal Heterostructures with Tetrapod Morphology. *Small* **2006**, *2*, 1454–1457.
47. Xia, Y. S.; Tang, Z. Y. Monodisperse Inorganic Supraparticles: Formation Mechanism, Properties and Applications. *Chem. Commun.* **2012**, *48*, 6320–6336.
48. Clapp, A. R.; Medintz, I. L.; Mauro, J. M.; Fisher, B. R.; Bawendi, M. G.; Mattoussi, H. Fluorescence Resonance Energy Transfer between Quantum Dot Donors and Dye-Labeled Protein Acceptors. *J. Am. Chem. Soc.* **2004**, *126*, 301–310.
49. Tang, Z. Y.; Kotov, N. A.; Giersig, M. Spontaneous Organization of Single CdTe Nanoparticles into Luminescent Nanowires. *Science* **2002**, *297*, 237–240.
50. Chen, H.; Lesnyak, V.; Bigall, N. C.; Gaponik, N.; Eychmüller, A. Self-Assembly of TGA-Capped CdTe Nanocrystals into Three-Dimensional Luminescent Nanostructures. *Chem. Mater.* **2010**, *22*, 2309–2314.
51. Zhou, D.; Lin, M.; Chen, Z. L.; Sun, H. Z.; Zhang, H.; Sun, H. C.; Yang, B. Simple Synthesis of Highly Luminescent Water-Soluble CdTe Quantum Dots with Controllable Surface Functionality. *Chem. Mater.* **2011**, *23*, 4857–4862.
52. Zhou, D.; Lin, M.; Liu, X.; Li, J.; Chen, Z. L.; Yao, D.; Sun, H. Z.; Zhang, H.; Yang, B. Conducting the Temperature-Dependent Conformational Change of Macrocyclic Compounds to the Lattice Dilation of Quantum Dots for Achieving an Ultrasensitive Nanothermometer. *ACS Nano* **2013**, *7*, 2273–2283.
53. Nair, P. V.; Thomas, K. G. Hydrazine-Induced Room-Temperature Transformation of CdTe Nanoparticles to Nanowires. *J. Phys. Chem. Lett.* **2010**, *1*, 2094–2098.
54. Zhang, H.; Wang, D. Y.; Yang, B.; Möhwald, H. Manipulation of Aqueous Growth of CdTe Nanocrystals to Fabricate Colloidally Stable One-Dimensional Nanostructures. *J. Am. Chem. Soc.* **2006**, *128*, 10171–10180.
55. Zhou, D.; Han, J. S.; Liu, Y.; Liu, M.; Zhang, X.; Zhang, H.; Yang, B. Nucleation of Aqueous Semiconductor Nanocrystals: A Neglected Factor for Determining the Photoluminescence. *J. Phys. Chem. C* **2010**, *114*, 22487–22492.
56. Dong, C. Powderx: Windows-95-Based Program for Powder X-ray Diffraction Data Processing. *J. Appl. Crystallogr.* **1999**, *32*, 838–838.
57. Niu, H. J.; Gao, M. Y. Diameter-Tunable CdTe Nanotubes Templated by 1D Nanowires of Cadmium Thiolate Polymer. *Angew. Chem., Int. Ed.* **2006**, *45*, 6462–6466.
58. Zhang, H.; Wang, D. Y. Controlling the Growth of Charged-Nanoparticle Chains through Interparticle Electrostatic Repulsion. *Angew. Chem., Int. Ed.* **2008**, *47*, 3984–3987.
59. Yuan, W.; Li, C. Y.; Zhao, C.; Sui, C. G.; Yang, W. T.; Xu, F. J.; Ma, J. Facilitation of Gene Transfection and Cell Adhesion by Gelatin-Functionalized PCL Film Surfaces. *Adv. Funct. Mater.* **2012**, *22*, 1835–1842.
60. Rück-Braun, K.; Petersen, M. Å.; Michalik, F.; Hebert, A.; Przyrembel, D.; Weber, C.; Ahmed, S. A.; Kowarik, S.; Weinelt, M. Formation of Carboxy- and Amide-Terminated Alkyl Monolayers on Silicon(111) Investigated by ATR-FTIR, XPS, and X-ray Scattering: Construction of Photoswitchable Surfaces. *Langmuir* **2013**, *29*, 11758–11769.
61. Zhou, Y. L.; Yang, M.; Sun, K.; Tang, Z. Y.; Kotov, N. A. Similar Topological Origin of Chiral Centers in Organic and Nanoscale Inorganic Structures: Effect of Stabilizer Chirality on Optical Isomerism and Growth of CdTe Nanocrystals. *J. Am. Chem. Soc.* **2010**, *132*, 6006–6013.
62. Zhang, H.; Wang, C. L.; Li, M. J.; Zhang, J. H.; Lu, G.; Yang, B. Fluorescent Nanocrystal-Polymer Complexes with Flexible Processability. *Adv. Mater.* **2005**, *17*, 853–857.
63. Wuister, S. F.; de Mello Donegá, C.; Meijerink, A. Influence of Thiol Capping on the Exciton Luminescence and Decay Kinetics of CdTe and CdSe Quantum Dots. *J. Phys. Chem. B* **2004**, *108*, 17393–17397.
64. Lee, J.; Sundar, V. C.; Heine, J. R.; Bawendi, M. G.; Jensen, K. F. Full Color Emission from II-VI Semiconductor Quantum Dot-Polymer Composites. *Adv. Mater.* **2000**, *12*, 1102–1105.
65. Zhang, H.; Wang, C. L.; Li, M. J.; Ji, X. L.; Zhang, J. H.; Yang, B. Fluorescent Nanocrystal-Polymer Composites from Aqueous Nanocrystals: Methods without Ligand Exchange. *Chem. Mater.* **2005**, *17*, 4783–4788.
66. Rogach, A. L.; Franzl, T.; Klar, T. A.; Feldmann, J.; Gaponik, N.; Lesnyak, V.; Shavel, A.; Eychmüller, A.; Rakovich, Y. P.; Donegan, J. F. Aqueous Synthesis of Thiol-Capped CdTe Nanocrystals: State-of-the-Art. *J. Phys. Chem. C* **2007**, *111*, 14628–14637.
67. Müller, M.; Kaiser, M.; Stachowski, G. M.; Resch-Genger, U.; Gaponik, N.; Eychmüller, A. Photoluminescence Quantum Yield and Matrix-Induced Luminescence Enhancement of Colloidal Quantum Dots Embedded in Ionic Crystals. *Chem. Mater.* **2014**, *26*, 3231–3237.
68. Demir, H. V.; Nizamoglu, S.; Erdem, T.; Mutlugun, E.; Gaponik, N.; Eychmüller, A. Quantum Dot Integrated LEDs Using Photonic and Excitonic Color Conversion. *Nano Today* **2011**, *6*, 632–647.
69. Han, J. S.; Luo, X. T.; Zhou, D.; Sun, H. Z.; Zhang, H.; Yang, B. Growth Kinetics of Aqueous CdTe Nanocrystals in the Presence of Simple Amines. *J. Phys. Chem. C* **2010**, *114*, 6418–6425.
70. Haugland, R. P. *Molecular Probes: The Handbook-A Guide to Fluorescent Probes and Labeling Technologies*; Invitrogen: Carlsbad, CA, 2010; Chapter 3.4.
71. Talapin, D. V.; Rogach, A. L.; Shevchenko, E. V.; Kornowski, A.; Haase, M.; Weller, H. Dynamic Distribution of Growth Rates within the Ensembles of Colloidal II-VI and III-V Semiconductor Nanocrystals as a Factor Governing Their Photoluminescence Efficiency. *J. Am. Chem. Soc.* **2002**, *124*, 5782–5790.
72. Davis, W.; Ohno, Y. Color Quality Scale. *Opt. Eng.* **2010**, *49*, 033602.
73. Qu, L. H.; Peng, X. G. Control of Photoluminescence Properties of CdSe Nanocrystals in Growth. *J. Am. Chem. Soc.* **2002**, *124*, 2049–2055.
74. Pradhan, N.; Battaglia, D. M.; Liu, Y. C.; Peng, X. G. Efficient, Stable, Small, and Water-Soluble Doped ZnSe Nanocrystal Emitters as Non-Cadmium Biomedical Labels. *Nano Lett.* **2007**, *7*, 312–317.
75. de Mello, J. C.; Wittmann, H. F.; Friend, R. H. An Improved Experimental Determination of External Photoluminescence Quantum Efficiency. *Adv. Mater.* **1997**, *9*, 230–232.